The Astronomical Journal, 124:1045–1053, 2002 August

RADIO CONTINUUM MAPS OF DEEPLY EMBEDDED PROTOSTARS: THERMAL JETS, MULTIPLICITY, AND VARIABILITY

Bo Reipurth,[1] Luis F. Rodríguez,[2] Guillem Anglada,[3,4] and John Bally[5]

Received 2002 February 25; accepted 2002 April 9

ABSTRACT

We have carried out a deep, 3.6 cm radio continuum survey of young outflow sources using the Very Large Array in its A configuration providing subarcsecond resolution. The seven regions observed are L1448-N, IRAS 2 and 4 in NGC 1333, L1551-NE, SSV 63 in L1630, HH 124 IRS in NGC 2264, and B335 IRS. The first three of these objects are known from submillimeter observations to be multiple sources, and we detect almost all known submillimeter components at 3.6 cm. The L1551-NE source is confirmed to be a subarcsecond binary. We find a third radio source in the SSV 63 system, which drives the multiple HH 24 jets. HH 124 IRS is embedded in a cometary cloud, where we detect a small cluster of six time-variable radio continuum sources. Six of the observed sources are resolved into compact thermal radio jets.

Key words: binaries: general — ISM: jets and outflows — radio continuum — stars: formation — stars: pre–main-sequence

1. INTRODUCTION

Outflow activity from young stars is strongly dependent on the stellar evolutionary stage, with the most powerful outflows emanating from the youngest Class 0 sources (see, e.g., Bontemps et al. 1996a). Such young sources are deeply embedded and usually only detectable at far-infrared and longer wavelengths. Radio continuum observations have emerged as a powerful tool to penetrate the huge extinctions of $A_V \sim 100$ often obscuring these sources. Concerted efforts have demonstrated that the sources of HH flows are almost always detectable at centimeter wavelengths (Bieging, Cohen, & Schwartz 1984; Rodríguez & Reipurth 1996, 1998), as are the sources of molecular outflows (see, e.g., Snell & Bally 1986; Anglada et al. 1998; Reipurth, Rodríguez, & Chini 1999a). The tremendous resolution offered by the Very Large Array (VLA) interferometer has permitted the discovery that some radio continuum sources can be resolved into tiny radio jets, normally with thermal spectra (Rodríguez et al. 1990; Rodríguez & Reipurth 1994; Rodríguez 1997) but occasionally with nonthermal spectra (Curiel et al. 1993; Wilner, Reid, & Menten 1999). Such observations provide unique information on conditions in the launch and collimation region of jets.

An additional aspect of high-resolution radio continuum observations is the possibility they offer to detect and resolve close binaries among the youngest stars, and a number of very young close binaries have been discovered this way (e.g., L1551 IRS5: Rodríguez et al. 1998; HH 111 IRS: Reipurth et al. 1999b; HH 7-11 SVS 13: Anglada, Rodríguez, & Torrelles 2000). This is particularly important in order to understand the binary frequency among deeply embedded outflow sources, which appears to be very high (Reipurth 2000). Furthermore, radio continuum observations enable a clearer picture of the small-scale clustering properties of embedded sources to be made.

In this paper we present sensitive, high-resolution observations at 3.6 cm of seven regions of recent star formation.

2. OBSERVATIONS

We have used the NRAO[6] Very Large Array in its A array configuration to observe seven regions containing deeply embedded protostars at 3.6 cm. The regions around NGC 1333/IRAS 2, NGC 1333/IRAS 4, L1551-NE, HH 24 IRS, and HH 124 IRS were observed on 2000 November 26, 27, 28, and 29. The region around L1448N was observed on 2000 November 26, 27, and 29. The region around B335 IRS was observed on 2001 January 6. In Table 1 we list the observational parameters for each region. Source properties and very accurate positions ($\sim 0\farcs05$) are listed in Table 2. There was no evidence of time variability in most of the regions observed on different days, and the flux densities given in Table 2 are the average over all the observations. However, some of the sources in the NGC 1333/IRAS 2 and HH 124 IRS regions exhibited rapid (over days) time variability, and they are discussed in detail below.

3. RESULTS

In the following we discuss the radio continuum detections in the seven regions observed in relation to the young objects already known to exist there.

3.1. *L1448-N* (*A, B*)

The L1448 cloud is part of the Perseus complex at a distance of 300 pc (Bachiller & Cernicharo 1986) and contains numerous signatures of outflow activity (see, e.g., Bachiller et al. 1990; Bally et al. 1997; Wolf-Chase, Barsony, &

[1] Institute for Astronomy, University of Hawaii, 2680 Woodlawn Drive, Honolulu, HI 96822; reipurth@ifa.hawaii.edu.
[2] Instituto de Astronomía, UNAM, Apdo. Postal 72-3 (Xangari), 58089 Morelia, Michoacán, Mexico; l.rodriguez@astrosmo.unam.mx.
[3] Instituto de Astrofisica de Andalucía, CSIC, Camino Bajo de Huétor 24, E-18008 Granada, Spain; guillem@iaa.es.
[4] Harvard-Smithsonian Center for Astrophysics, 60 Garden Street, MS-42, Cambridge, MA 02138.
[5] Center for Astrophysics and Space Astronomy, University of Colorado, Boulder, CO 80309; bally@casa.colorado.edu.

[6] The National Radio Astronomy Observatory is a facility of the National Science Foundation operated under cooperative agreement by Associated Universities, Inc.

TABLE 1
REGIONS OBSERVED AT 3.6 cm

Region	Phase Center		Phase Calibrator	Bootstrapped Flux Density (Jy)	rms Noise (μJy)	Synthesized Beam		Time[a] (hr)
	α (J2000.0)	δ (J2000.0)				Size (arcsec)	P.A. (deg)	
L1448-N	03 25 36.4	30 45 18	0336+323	1.675 ± 0.013	13	0.31 × 0.27	69	3
NGC 1333/IRAS 2	03 29 11.2	31 13 20	0336+323	1.674 ± 0.013	9	0.30 × 0.27	71	6
NGC 1333/IRAS 4	03 29 11.2	31 13 20	0336+323	1.674 ± 0.013	7	0.30 × 0.27	84	10
L1551-NE	04 31 44.4	18 08 32	0449+113[b]	1.368 ± 0.057	8	0.34 × 0.27	57	10
SSV 63	05 46 08.2	−00 10 17	0552+032	0.710 ± 0.016	9	0.35 × 0.30	32	6
HH 124	06 41 03.2	10 15 04	0613+131	0.395 ± 0.002	7	0.31 × 0.30	45	10
B335 IRS	19 37 00.8	07 34 11	1950+081	0.809 ± 0.005	8	0.32 × 0.28	−33	8

NOTE.—Units of right ascension are hours, minutes, and seconds, and units of declination are degrees, arcminutes, and arcseconds.
[a] Total observing time.
[b] This phase calibrator exhibited small but significant flux density variations over the four observing sessions.

O'Linger 2000; Eislöffel 2000). The northern part of the cloud contains the source IRS 3, which is now known to consist of three individual sources, N-A, N-B, and NW. Source L1448-N was detected at centimeter wavelengths by Anglada et al. (1989) and subsequently resolved into two components (N-A and N-B) by Curiel et al. (1990) in low-resolution 2 and 6 cm VLA maps. Both of these objects are Class 0 sources and drive outflows. Barsony et al. (1998) suggest that source B has a higher luminosity (7 $L_{\odot}$) than source A (1 $L_{\odot}$). The source NW was first noted by Terebey & Padgett (1997) in the 2.7 mm continuum and is also a Class 0 source (Shirley et al. 2000).

In Figure 1 we show our high-resolution 3.6 cm map of the northern part of L1448. Source A (Fig. 2) is by far the most prominent source, despite its possibly lower luminosity. It deconvolves to $(0\farcs17 \pm 0\farcs02) \times (0\farcs12 \pm 0\farcs02)$ at a P.A. of $104° \pm 14°$, which we interpret as a thermal radio jet. The deconvolved dimensions of this and other angularly resolved sources in the present study are listed in Table 3. These deconvolved dimensions are corrected for the usually small effects of bandwidth smearing. Wolf-Chase et al. (2000) suggest the presence of a redshifted CO outflow lobe from source A at a P.A. of about 150°, although multiple overlapping outflows make it difficult to unambiguously

TABLE 2
PARAMETERS OF THE 3.6 cm VLA SOURCES

Object	Position		Separation[a] (arcsec)	Flux[b] (mJy)	Distance (pc)
	α (J2000.0)	δ (J2000.0)			
L1448N-A	03 25 36.493	30 45 21.97	...	1.19	300
L1448N-B	03 25 36.309	30 45 15.04	7.3	0.23	300
L1448N-NW	03 25 35.660	30 45 34.19	16.3	0.18	300
L1448-C	03 25 38.867	30 44 05.34	82.5	0.23	300
NGC 1333/IRAS 2A	03 28 55.560	31 14 37.17	...	0.22	310
NGC 1333/IRAS 2B	03 28 57.370	31 14 15.90	31.5	0.37	310
NGC 1333–VLA 2	03 29 01.970	31 15 38.22	102.4	2.89	310
NGC 1333/IRAS 2–VLA 9	03 28 57.216	31 14 19.11	27.9	0.12	310
NGC 1333–VLA 12	03 28 59.835	31 14 02.83	64.7	0.23	310
NGC 1333/IRAS 4A1	03 29 10.529	31 13 31.05	...	0.32	310
NGC 1333/IRAS 4A2	03 29 10.421	31 13 32.21	1.8	0.11	310
NGC 1333/IRAS 4B	03 29 12.003	31 13 08.14	29.7	0.33	310
NGC 1333/IRAS 4C	03 29 13.539	31 13 58.33	47.3	0.11	310
L1551–NE-A	04 31 44.497	18 08 31.67	...	0.39	140
L1551–NE-B	04 31 44.465	18 08 31.88	0.5	0.27	140
SSV 63–E	05 46 08.485	−00 10 03.03	...	0.27	460
SSV 63–W	05 46 07.857	−00 10 01.22	9.6	0.07	460
SSV 63–NE	05 46 08.922	−00 09 56.10	9.5	0.05	460
HH 24 MMS	05 46 08.329	−00 10 43.39	40.4	0.17	460
HH 124 VLA 1	06 41 02.598	10 15 03.60	...	0.07	800
HH 124 VLA 2	06 41 03.528	10 15 06.36	14.0	0.15	800
HH 124 VLA 7	06 41 01.217	10 14 50.28	24.3	0.12	800
HH 124 VLA 8	06 41 01.531	10 14 56.01	17.5	0.13	800
HH 124 VLA 9	06 41 02.647	10 15 01.94	1.8	0.12	800
HH 124 VLA 10	06 41 04.465	10 14 52.57	29.7	0.10	800
B335 IRS	19 37 00.888	07 34 09.84	...	0.39	250

[a] Distance to first component.
[b] Total flux density corrected for primary beam response.

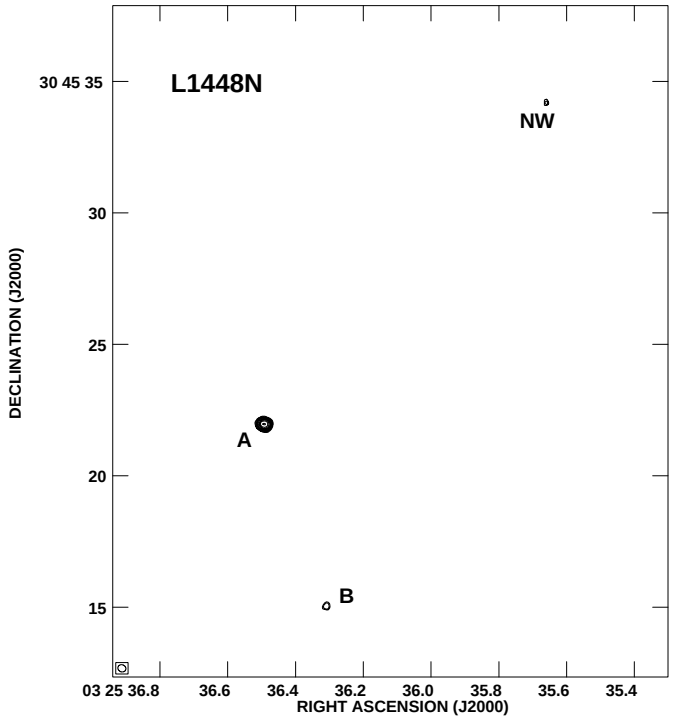

FIG. 1.—L1448-N region as seen in a natural-weight VLA image at 3.6 cm wavelength. The half-power contour of the beam is shown in the bottom left-hand corner. Contour levels are −5, 5, 6, 8, 10, 12, 15, 20, 30, 40, and 60 times 13 μJy, the rms noise of the image.

assign any given outflow feature to a specific source. Girart & Accord (2001) detected a well-collimated SiO flow along an axis passing through source B at a P.A. of about 110°. This is very close to the P.A. of 104° measured for our thermal radio jet around source A, suggesting that this is another case of almost parallel outflows from nearby newborn stars.

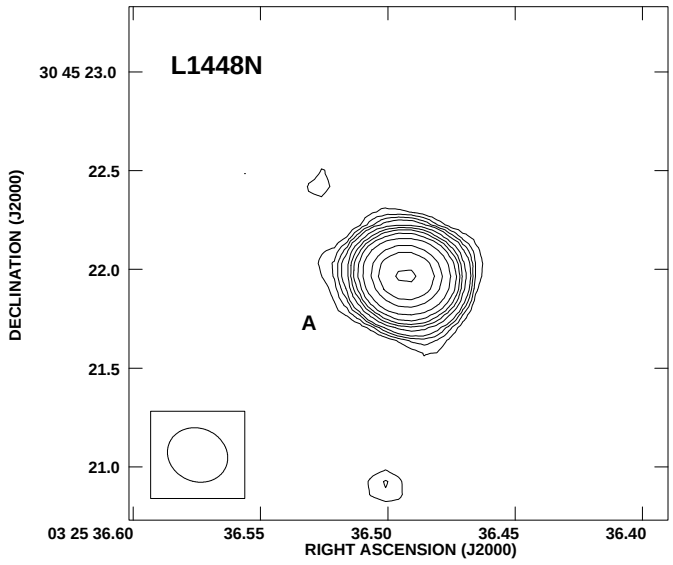

FIG. 2.—L1448N-A source as seen in a natural-weight VLA image at 3.6 cm wavelength. The image parameters are as in Fig. 1, except that the contours are −3, 3, 4, 5, 6, 8, 10, 12, 15, 20, 30, 40, and 60 times the rms noise.

TABLE 3
PARAMETERS OF RESOLVED VLA SOURCES

Object	Deconvolved Size (arcsec)	P.A. (deg)
L1448N-A	$(0.17 \pm 0.02) \times (0.12 \pm 0.02)$	104 ± 14
NGC 1333–VLA 2	$(0.38 \pm 0.02) \times (0.14 \pm 0.03)$	176 ± 4
NGC 1333/IRAS 4A1	$(0.42 \pm 0.03) \times (0.28 \pm 0.03)$	92 ± 11
L1551–NE-A	$(0.23 \pm 0.02) \times (0.14 \pm 0.02)$	48 ± 10
L1551–NE-B	$(0.37 \pm 0.03) \times (0.21 \pm 0.03)$	58 ± 8
B335 IRS	$(0.25 \pm 0.03) \times (0.16 \pm 0.03)$	87 ± 15

We also detected L1448-C to the south of L1448-N. It appears as an unresolved source, and its parameters are given in Table 2.

3.2. *NGC 1333/IRAS 2*

The NGC 1333 region was studied at 50 and 100 μm with the *IRAS* Chopped Photometric Channel by Jennings et al. (1987). They detected a source, labeled NGC 1333/IRAS 2, also known as IRAS 03258+3104 in the Point Source Catalogue, with a far-infrared luminosity of 34 $L_{\odot}$, assuming a distance of 310 pc (for a discussion of the distance to NGC 1333 and the Perseus clouds, see Herbig 1998, de Zeeuw et al. 1999, and Getman et al. 2002). In their millimeter study of NGC 1333, Liseau, Sandell, & Knee (1988) found a molecular outflow from IRAS 2. Sandell et al. (1994) detected a submillimeter continuum source at the location of IRAS 2 and a quadrupolar molecular outflow centered on the source, suggesting that it must be a binary. Neither the near-infrared observations of Hodapp & Ladd (1995) nor the higher resolution 1.3 mm maps of Lefloch et al. (1998) detected a binary at IRAS 2, but Blake (1997) found two sources, IRAS 2A and 2B, at 2.7 mm, both of which were detected by Rodríguez, Anglada, & Curiel (1999) on low-resolution maps at 3.6 and 6 cm (IRAS 2A = VLA 7 and IRAS 2B = VLA 10). Additionally, the latter authors pointed out that the H_2 observations of Hodapp & Ladd (1995) and SiO maps of Blake (1997) suggest that the quadrupolar flow may originate from IRAS 2A, which therefore itself might be a binary.

In Figure 3 we show our high-resolution VLA-A map of the IRAS 2 region. Both IRAS 2A = VLA 7 and IRAS 2B = VLA 10 have been detected and showed no variability either during the four days of observations or with respect to earlier lower resolution observations. A third source suddenly appeared on the last day of observations and coincides precisely with the unrelated foreground star BD +30°547 located 4″ to the northwest of IRAS 2B. The source was already detected (their source VLA 9) by Rodríguez et al. (1999), who also noted its variable nature. During this day (2000 November 29), VLA 9 showed significant variation on a timescale of hours (see Fig. 4). We did not detect linear or circular polarization from this source at a 4 σ upper limit of ~20%. We tentatively identify the time-variable radio emission as synchrotron emission from an active stellar magnetosphere (Feigelson & Montmerle 1999; Rodríguez et al. 1999).

Within our angular resolution neither IRAS 2A nor 2B show any evidence for being extended; in particular we note that the possible binary nature of IRAS 2A could not be confirmed, suggesting that if it is a binary and if both com-

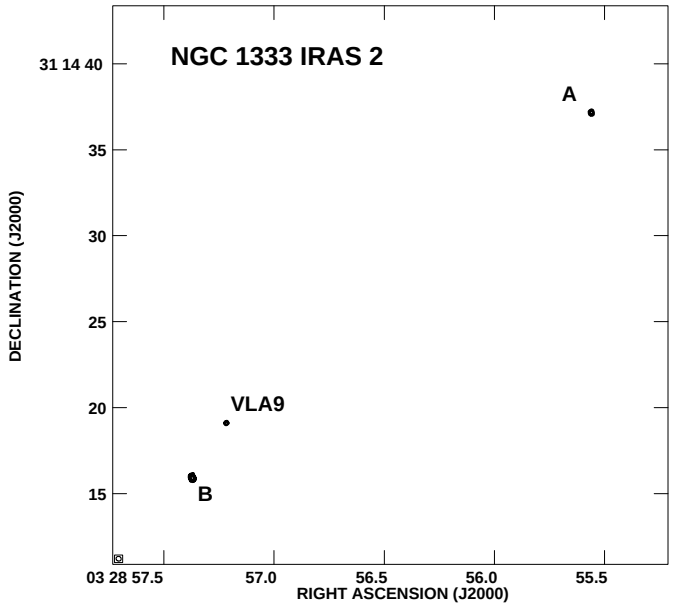

FIG. 3.—NGC 1333 IRAS 2 region as seen in a natural-weight VLA image at 3.6 cm wavelength. Contours are as in Fig. 1, except that the levels are in units of 9 μJy, the rms noise of the image.

ponents were bright enough at the time of our observations to be detected, then the projected separation must be less than 0.″3, or ~93 AU at a distance of 310 pc. No circular or linear polarization was detected in any of the sources. In Table 2 we provide the most accurate positions so far of the embedded IRAS 2A and 2B sources. Our very accurate radio position of VLA 9 can be compared with the optical position of BD +30°547 to give an estimate of how well the radio and optical coordinate systems in this region of the sky are registered. We find that our radio position and the optical position of BD +30°547 given in the Tycho Reference Catalogue (Høg et al. 1998) coincide to better than 0.″1.

We also detected the source VLA 2 of Rodríguez et al. (1997, 1999). VLA 2 is associated with the source MMS 3 (Chini et al. 1997; Bachiller et al. 1998). Our image (see Fig. 5) shows that the source itself is extended in the north-south direction (see Table 3) and that it also has a faint extended jet in the same direction. The bipolar thermal radio jet from VLA 2 has an angular extent of 4″, corresponding to about 1240 AU. The jet shows evidence for dramatic wiggling. If the individual knots were ejected ballistically, they should spread out in a precession cone, but this is not seen. Rather, it appears that the flow remains narrow despite the internal wiggling. This suggests that a mechanism exists that somehow confines the outflow to a much narrower jet than it would have been under purely ballistic motion in a precession cone. We note that this new radio jet points toward HH 12 and is a possible driving source for this large HH object.

Finally, we also detected the source VLA 12 of Rodríguez et al. (1999), who suggested that it is an extragalactic source.

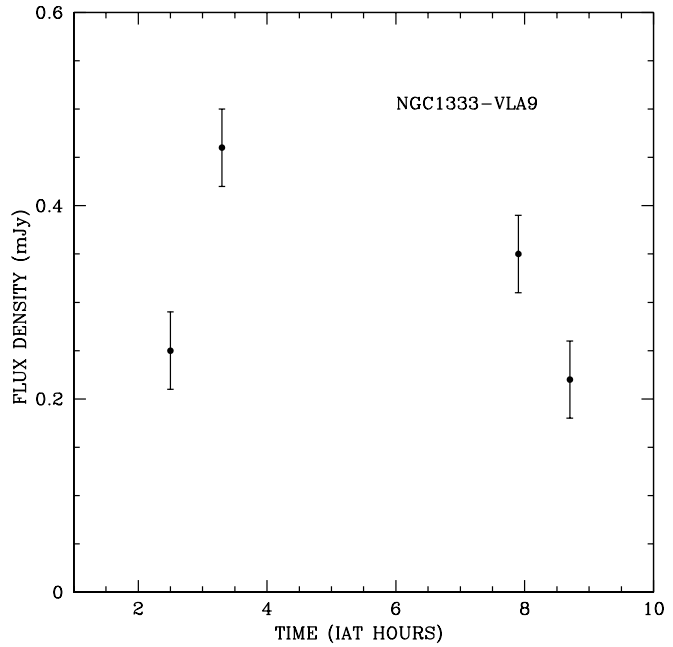

FIG. 4.—Flux density as a function of time for NGC 1333 VLA 9, during 2000 November 29.

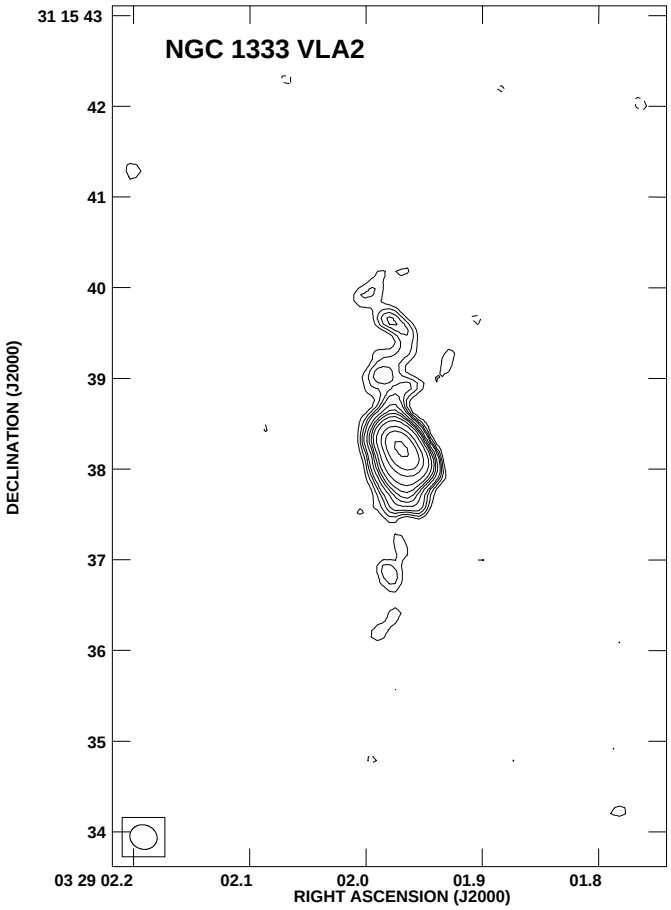

FIG. 5.—Source VLA 2 in the NGC 1333 region as seen in a natural-weight VLA image at 3.6 cm wavelength. Note the extensions in the north-south direction. The half-power contour of the beam is shown in the bottom left-hand corner. Contour levels are −3, 3, 4, 5, 6, 8, 10, 12, 15, 20, 30, 40, and 60 times 12 μJy, the rms noise in this part of the image, after correction for the primary beam response.

3.3. *NGC 1333/IRAS 4*

First detected by Jennings et al. (1987), NGC 1333/IRAS 4 has attracted much attention after Sandell et al. (1991), using submillimeter observations, found that it forms a protostellar binary system, 4A and 4B, with a more distant third component (labeled 4C by Rodríguez et al. 1999). All of these three submillimeter sources were detected in low-resolution radio continuum maps by Mundy et al. (1993; A and B) and Rodríguez et al. (1999; A, B, and C). Lay, Carlstrom, & Hills (1995) performed submillimeter interferometry of the A-B binary and found that the visibility curve of 4A was consistent with a 1″.8 binary and also suggested higher multiplicity for 4B. Looney, Mundy, & Welch (2000) resolved the 4A binary in their continuum maps at 2.7 mm.

We show our high-resolution 3.6 cm map of the IRAS 4A, 4B, and 4C regions in Figure 6. Both components of the 4A binary have been detected with a separation of 1″.8 at a P.A. of -50°, in excellent agreement with the results of Lay et al. (1995) and Looney et al. (2000). The southeastern component, which is the brightest at 2.7 mm and is designated 4A1 by Looney et al. (2000), also has the larger flux at 3.6 cm, being a factor of 3 brighter than the companion 4A2. Accurate positions for the sources are listed in Table 2. The bright component 4A1 of this double deconvolves to $(0''.42 \pm 0''.03) \times (0''.28 \pm 0''.03)$ at a P.A. of $92^\circ \pm 11^\circ$, probably because of a thermal radio jet (see Fig. 7). The main molecular outflow detected from the 4A source runs along a mostly northeast-southwest axis (Blake et al. 1995; Lefloch et al. 1998), and a fainter outflow detected in HCN by Choi (2001) has a lobe to the south of 4A, so it is not clear how the radio jet from the 4A1 component is linked to these other outflow tracers.

Source 4B was found to be a 10″ binary oriented east-west by Choi, Panis, & Evans (1999), Looney et al. (2000), Smith et al. (2000), and di Francesco et al. (2001). However, we do not find any evidence for such a companion to 4B, and we conclude that, at least at the time of our observations, it does not emit strongly in the radio continuum.

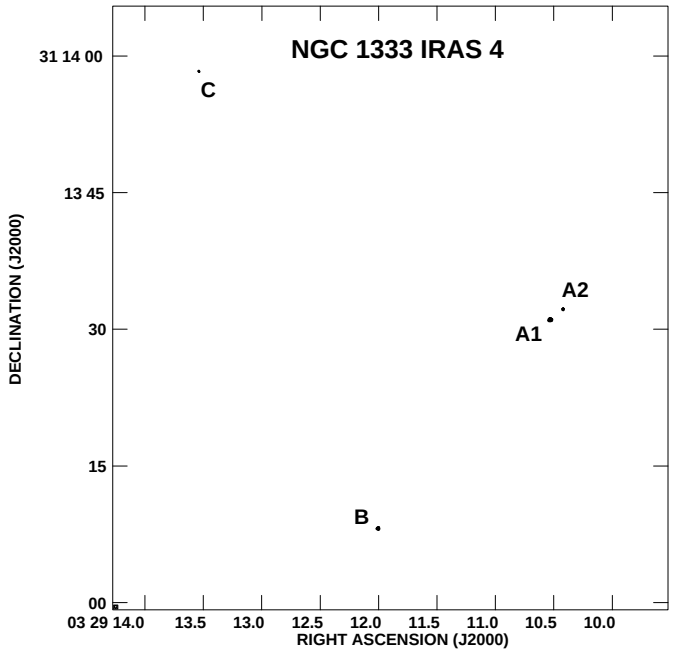

FIG. 6.—NGC 1333 IRAS 4 region as seen in a natural-weight VLA image at 3.6 cm wavelength. Contours are as in Fig. 1, except that the levels are in units of 7 μJy, the rms noise of the image.

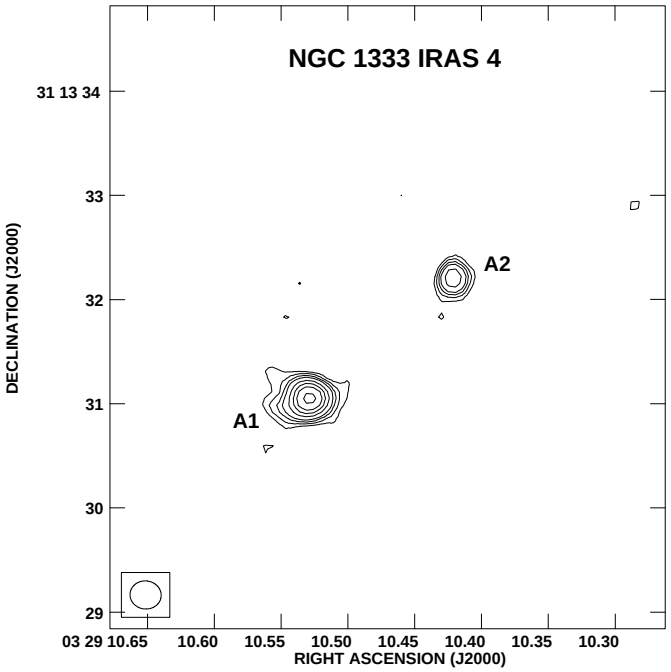

FIG. 7.—NGC 1333 IRAS 4A region as seen in a natural-weight VLA image at 3.6 cm wavelength. Contours are as in Fig. 5, except that the levels are in units of 7 μJy, the rms noise of the image.

Source 4C was also detected in our 3.6 cm map (see Fig. 6), and it appears unresolved. We note in passing that there is some confusion in the literature as to the designation of this source. We follow Rodríguez et al. (1999), Smith et al. (2000), Choi (2001), di Francesco et al. (2001), and Sandell & Knee (2001) in calling this source 4C but note that the companion to source 4B was labeled 4C by Choi et al. (1999) and Looney et al. (2000).

3.4. *L1551-NE*

The L1551-NE source in Taurus was discovered at far-infrared wavelengths by Emerson et al. (1984). In the optical only a minor reflection nebula is visible, but in the near-infrared a much larger reflection nebula emerges (Hodapp & Ladd 1995). The source is likely to drive the well-known HH objects HH 28 and HH 29 and a small chain of HH knots, HH 454, surrounding the source (Devine, Reipurth, & Bally 1999) as well as a finely collimated infrared [Fe II] jet that emanates from the source along the well-defined axis of these HH objects (Reipurth et al. 2000).

The L1551-NE source was detected at 3.6 cm by Rodríguez, Anglada, & Raga (1995), who found evidence that it may be a binary, but the noise in the data made the detection of binarity somewhat ambiguous. We here present high-resolution, high signal-to-noise ratio 3.6 cm maps that affirm that L1551-NE is indeed a binary with a separation of 0″.5 at a P.A. of 297° (Fig. 8). At 3.6 cm the SE component (here called A) is the brighter, whereas the NW component (B) is a factor of $\sim$0.7 fainter. In their infrared *Hubble Space Telescope* study of the source, Reipurth et al. (2000) found a cone-shaped cavity and a finely collimated [Fe II] jet but noted that the brightest point of the compact cometary

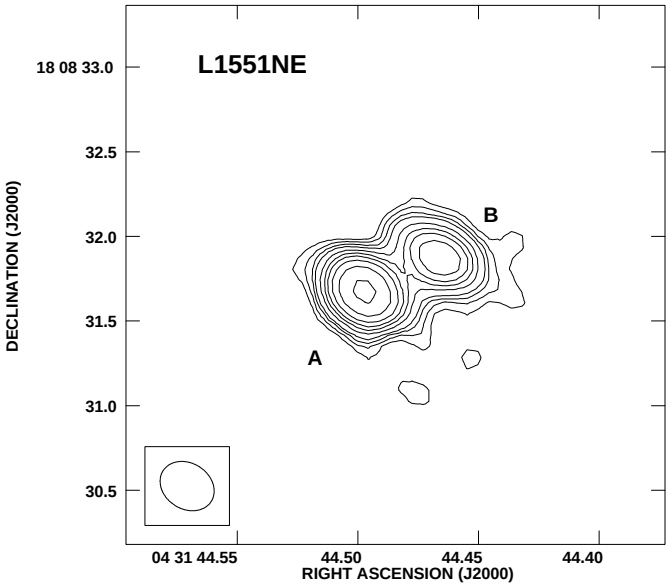

FIG. 8.—L1551-NE binary source as seen in a natural-weight VLA map at 3.6 cm wavelength. Contours are as in Fig. 5, except that the levels are in units of 8 μJy, the rms noise of the image.

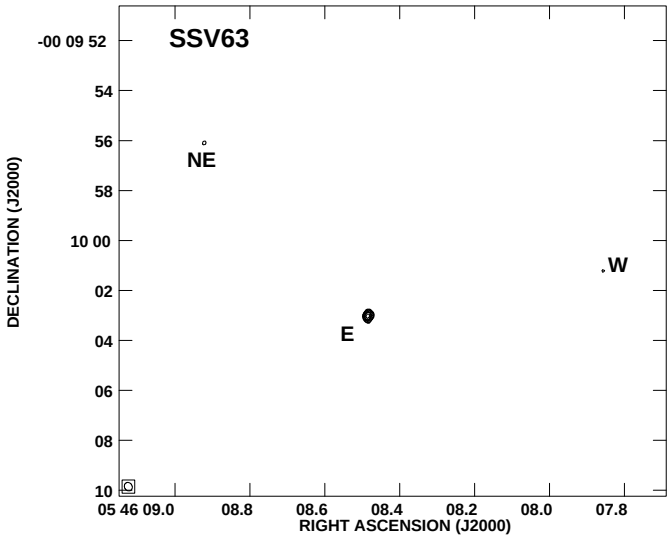

FIG. 9.—SSV 63 region with the sources E, W, and NE, as seen in a natural-weight VLA map at 3.6 cm wavelength. Contours are as in Fig. 1, except that the levels are in units of 9 μJy, the rms noise of the image.

nebula is offset by 0.″2 from the axis of the jet. This can be understood now since the orientation of the binary strongly suggests that the jet emanates from component A, whereas the peak brightness of the cometary nebula is due to component B.

Both sources are angularly resolved, and their deconvolved sizes are given in Table 3. We interpret these two extended sources as thermal radio jets and note that their outflow axes are approximately aligned in the sky, with component A elongated along P.A. $= 228° \pm 10°$ and component B along P.A. $= 238° \pm 8°$. This is very close to the axis of the optical bipolar HH 454 flow surrounding L1551-NE, which is 242° (Devine et al. 1999), and the infrared [Fe II] jet emanating from component A, which has P.A. $= 243°$ (Reipurth et al. 2000). It is noteworthy that the two distant bow shocks HH 29 and HH 28 have position angles with respect to L1551-NE of 242° and 240°, respectively. The ages of these two bow shocks are 1900 and 4000 yr, respectively, compared to the age of the thermal radio jets, which are of the order of 2 yr, assuming the same tangential motions ($\sim$100 km s^{-1}) as the optical bow shocks (Devine et al. 1999). In other words, it appears that the flow axis of the driving source has remained virtually the same, within the measurement errors, for the past several thousand years. A similarly stable outflow axis is found for the giant HH 111 flow (Reipurth et al. 1999b).

We note that the 1.3 mm continuum source detected by Moriarty-Schieven et al. (2000) about 1.″4 southeast of the VLA binary was not detected in our maps.

3.5. *SSV 63*

The HH 24 region comprises several well-collimated jets (see, e.g., Eislöffel & Mundt 1997), originating in the vicinity of the near-infrared double source SSV 63. SSV 63E is the brighter at 2.2 μm, with SSV 63W about 10″ farther to the west. Additionally, an infrared reflection nebula lies to the northeast of SSV 63. *JHK* images of the region are shown by Moneti & Reipurth (1995), which demonstrates that SSV 63NE consists of two separate nebulae, NE-1 and NE-2. Davis et al. (1997) found that SSV 63W is a binary with 2″ separation, and Terquem et al. (1999) suggested that SSV 63E may be a close triple system. Bontemps, André, & Ward-Thompson (1995) and Bontemps, Ward-Thompson, & André (1996b) detected both SSV 63E and SSV 63W at 2, 3.6, and 6 cm (their sources 6 and 3, respectively). Further 3.6 and 6 cm measurements of the two sources are given by Anglada et al. (1998).

We detect three sources in our 3.6 cm map of the region (Fig. 9). The bright source corresponds to SSV 63E, and also SSV 63W is detected 9.″7 farther west. None of these sources show any further components, so we cannot corroborate their suggested binarity/multiplicity. We further detect a third source 9.″6 to the northeast of SSV 63E, located close to the base of the SSV 63NE-1 reflection nebula. There has been some doubt as to whether SSV 63E could be the source of this nebulosity or if it is illuminated by its own source. Our detection of a source at the apex of the NE-1 nebula strongly suggests that it has its own illuminating source.

The source SSV 63E appears to be extended, and we estimate an angular diameter of 0.″3. However, we were unable to obtain a robust deconvolution for its dimensions and do not include it in Table 3.

Chini et al. (1993) discovered a Class 0 source, HH 24 MMS, south of SSV 63. This source was weakly detected at low resolution at 3.6 and 6 cm by Bontemps et al. (1996b). In our original map we did not detect a counterpart to HH 24 MMS above a 5 σ level. However, closer inspection of the image suggested the presence of a faint, extended source at the position of HH 24 MMS. An image made with taper to smooth the angular resolution to $\sim$1″ (see Fig. 10) unambiguously shows the source, whose parameters are included in Table 2. This source is clearly extended, with angular dimension of order 1″. Our flux density is, within errors, in agreement with the lower resolution data of Bontemps et al. (1996b).

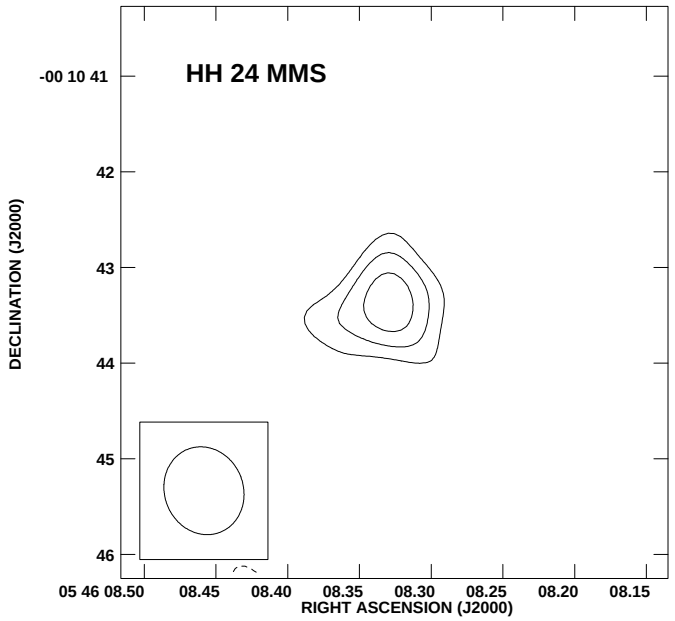

FIG. 10.—HH 24 MMS source as seen in a natural-weight VLA map at 3.6 cm wavelength. This image has a (u, v) taper of 200 kλ and the synthesized beam is $0\farcs93 \times 0\farcs82$ with P.A. $= 21°$. Contours are as in Fig. 5, except that the levels are in units of 13 μJy, the rms noise in this part of the image, after correction for the primary beam response.

3.6. *HH 124 IRS*

The IRAS source 06382+1017 is embedded in a small cometary-shaped cloud that is located just north of the NGC 2264 cluster and facing toward it. It has a luminosity of about 90 $L_\odot$ and was detected at near-infrared wavelengths by Piché, Howard, & Pipher (1995) and Moneti & Reipurth (1995) and at 1300 μm by Reipurth et al. (1993). It is centered at the middle of the axis of the giant HH 124 outflow (Walsh, Ogura, & Reipurth 1992; Ogura 1995). More recently, Reipurth et al. (2002) have found that yet another giant HH flow, HH 571/572, emerges from the source region. In a low-resolution VLA study, Rodríguez & Reipurth (1998) mapped the region at 3.6 cm and found two sources within the *IRAS* uncertainty ellipse, separated by $13\farcs5$, which at the assumed distance of 800 pc corresponds to a projected separation of 10,800 AU.

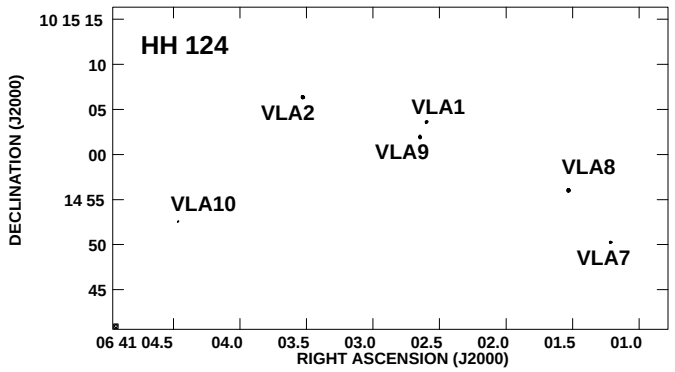

FIG. 11.—HH 124 region as seen in a natural-weight VLA map at 3.6 cm wavelength. Contours are as in Fig. 1, except that the levels are in units of 7 μJy, the rms noise of the image.

TABLE 4

FLUX DENSITIES OF RADIO SOURCES NEAR HH 124 IRS

Object	2000 Nov 26	2000 Nov 27	2000 Nov 28	2000 Nov 29
HH 124 VLA 1	0.07	0.05	0.11	0.08
HH 124 VLA 2	0.11	0.16	0.18	0.12
HH 124 VLA 7	0.18	0.09	0.09	0.11
HH 124 VLA 8	0.13	0.18	0.08	0.16
HH 124 VLA 9	0.11	0.11	0.22	0.08
HH 124 VLA 10	0.11	0.06	0.10	0.14

NOTE.—Flux densities are given in units of mJy. Error in flux density is $\sim$0.01 mJy.

Our deep 3.6 cm map reveals a small compact cluster of six sources centered on IRAS 06382+1017 (Fig. 11). Two of these sources, VLA 1 and VLA 2, were detected previously by Rodríguez & Reipurth (1998), together with four background sources, VLA 3–6. The other four are new detections, which we label VLA 7–10. Interestingly, all these sources (VLA 1, 2, and 7–10) show day-to-day variations through the 4 days covering our observations, strongly suggesting that they are Galactic sources, and probably all are located within the cometary cloud. In Table 4 we list the flux densities of these sources over the four epochs observed. A similar cluster of time-variable radio sources has been found in the GGD 14 region (Gómez, Rodríguez, & Garay 2000, 2002). As in the case of the radio source associated with BD $+30°547$, we tentatively attribute the emission to gyrosynchrotron radiation from an active stellar magnetosphere. We did not find linear or circular polarization in any of these sources. However, given the relative weakness of the sources, the polarization upper limits are not stringent ($\leq$50%). All six sources appear as unresolved in our images. With a largest dimension of $48''$, the little cluster spreads across 0.2 pc. A new wide-field CCD survey of the region has identified a number of new HH flows apparently origi-

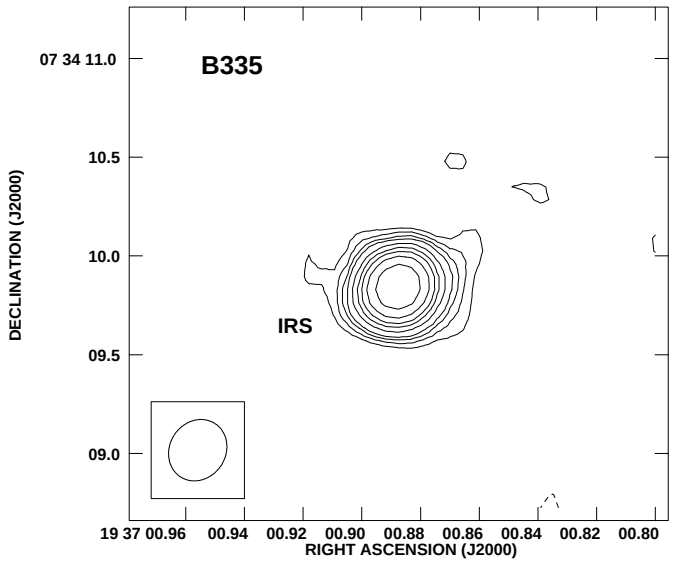

FIG. 12.—B335 IRS source as seen in a natural-weight VLA map at 3.6 cm wavelength. Contours are as in Fig. 5, except that the levels are in units of 8 μJy, the rms noise of the image.

nating in the dense, cometary cloud, testifying to the likely youth of the sources (Reipurth et al. 2002).

3.7. *B335 IRS*

The isolated Bok globule B335 provides the prototypical case of isolated star formation and has been studied at many wavelengths. A deeply embedded source is located at the center of the globule and is detected at far-infrared and submillimeter wavelengths (Keene et al. 1983). Outflow activity is detected at millimeter, optical, and infrared wavelengths (Cabrit, Goldsmith, & Snell 1988; Reipurth, Heathcote, & Vrba 1992; Hodapp 1998) and follows a well-defined axis oriented east-west. High-resolution millimeter observations show that $C^{18}O$ and 1.2 mm dust continuum emission is elongated perpendicular to the outflow axis (Chandler & Sargent 1993; Wilner et al. 2000). The source was detected at 3.6 cm by Anglada et al. (1992).

Our new high-resolution 3.6 cm map shows no evidence for any companions within our resolution. The source is clearly elongated in the east-west direction, with deconvolved dimensions of $(0\farcs25 \pm 0\farcs03) \times (0\farcs16 \pm 0\farcs03)$ at a P.A. of $87° \pm 15°$ (Fig. 12). In view of the good alignment with the outflow axis defined at other wavelengths, we interpret this as evidence for a compact thermal radio jet.

The total flux density of the source in our map is twice as large as the detection of Anglada et al. (1992), suggesting considerable variability of this source over a timescale of years. Avila, Rodríguez, & Curiel (2001) do not detect this source in their 1994 observations and also suggest that it is time variable.

4. CONCLUSIONS

We have used the VLA in its high-resolution A configuration to study seven regions of recent star birth at 3.6 cm, namely, L1448-N, NGC 1333 IRAS 2 and IRAS 4, L1551-NE, SSV 63 in L1630, HH 124 in NGC 2264, and B335. We have detected almost all known, deeply embedded, protostellar objects within our maps as well as several hitherto unknown sources. The data offer new insights into the presence, direction, and structure of compact thermal radio jets from these newborn stars. In one case, L1551-NE, our maps resolve the source into a $0\farcs5$ close binary. In a number of sources we are detecting pronounced variability in the radio continuum emission. The data provide further illustration of the power and usefulness of studying star-forming regions with the VLA interferometer.

We thank an anonymous referee for a helpful report. G. A. acknowledges partial support from MCYT grant PB 98-0670-C02, from Junta de Andalucía, and from MEC, Spain, and from SAO, US.

REFERENCES

Anglada, G., Rodríguez, L. F., Cantó, J., Estalella, R., & Torrelles, J. M. 1992, ApJ, 395, 494
Anglada, G., Rodríguez, L. F., & Torrelles, J. M. 2000, ApJ, 542, L123
Anglada, G., Rodríguez, L. F., Torrelles, J. M., Estalella, R., Ho, P. T. P., Cantó, J., López, R., & Verdes-Montenegro, L. 1989, ApJ, 341, 208
Anglada, G., Villuendas, E., Estalella, R., Beltrán, M. T., Rodríguez, L. F., Torrelles, J. M., & Curiel, S. 1998, AJ, 116, 2953
Avila, R., Rodríguez, L. F., & Curiel, S. 2001, Rev. Mexicana Astron. Astrofis., 37, 201
Bachiller, R., & Cernicharo, J. 1986, A&A, 168, 262
Bachiller, R., Cernicharo, J., Martin-Pintado, J., Tafalla, M., & Lazareff, B. 1990, A&A, 231, 174
Bachiller, R., Guilloteau, S., Gueth, F., Tafalla, M., Dutrey, A., Codella, C., & Castets, A. 1998, A&A, 339, L49
Bally, J., Devine, D., Alten, V., & Sutherland, R. S. 1997, ApJ, 478, 603
Barsony, M., Ward-Thompson, D., André, P., & O'Linger, J. 1998, ApJ, 509, 733
Bieging, J. H., Cohen, M., & Schwartz, P. R. 1984, ApJ, 282, 699
Blake, G. A. 1997, in IAU Symp. 178, Molecules in Astrophysics, Probes and Processes, ed. E. F. van Dishoeck (Dordrecht: Kluwer), 31
Blake, G. A., Sandell, G., van Dieshoeck, E. F., Groesbeck, T. D., Mundy, L. G., & Aspin, C. 1995, ApJ, 441, 689
Bontemps, S., André, P., Terebey, S., & Cabrit, S. 1996a, A&A, 311, 858
Bontemps, S., André, P., & Ward-Thompson, D. 1995, A&A, 297, 98
Bontemps, S., Ward-Thompson, D., & André, P. 1996b, A&A, 314, 477
Cabrit, S., Goldsmith, P. F., & Snell, R. L. 1988, ApJ, 334, 196
Chandler, C. J., & Sargent, A. I. 1993, ApJ, 414, L29
Chini, R., Krügel, E., Haslam, C. G. T., Kreysa, E., Lemke, R., Reipurth, B., Sievers, A., & Ward-Thompson, D. 1993, A&A, 272, L5
Chini, R., Reipurth, B., Sievers, A., Ward-Thompson, D., Haslam, C. G. T., Kreysa, E., & Lemke, R. 1997, A&A, 325, 542
Choi, M. 2001, ApJ, 553, 219
Choi, M., Panis, J.-F., & Evans, N. J. 1999, ApJS, 122, 519
Curiel, S., Raymond, J. C., Rodríguez, L. F., Cantó, J., & Moran, J. M. 1990, ApJ, 365, L85
Curiel, S., Rodríguez, L. F., Moran, J. M., & Cantó, J. 1993, ApJ, 415, 191
Davis, C. J., Ray, T. P., Eislöffel, J., & Corcoran, D. 1997, A&A, 324, 263
Devine, D., Reipurth, B., & Bally, J. 1999, AJ, 118, 972
de Zeeuw, P. T., Hoogerwerf, R., de Bruijne, J. H. J., Brown, A. G. A., & Blaauw, A. 1999, AJ, 117, 354
di Francesco, J., Myers, P. C., Wilner, D. J., Ohashi, N., & Mardones, D. 2001, ApJ, 562, 770
Eislöffel, J. 2000, A&A, 354, 236
Eislöffel, J., & Mundt, R. 1997, AJ, 114, 280
Emerson, J. P., Harris, S., Jennings, R. E., Beichman, C. A., Baud, B., Beintema, D. A., Marsden, P. L., & Wesselius, P. R. 1984, ApJ, 278, L49
Feigelson, E. D., & Montmerle, T. 1999, ARA&A, 37, 363
Getman, K., Feigelson, E. D., Townsley, L., Bally, J., Lada, C. J., & Reipurth, B. 2002, ApJ, in press
Girart, J. M., & Acord, J. M. P. 2001, ApJ, 552, L63
Gómez, Y., Rodríguez, L. F., & Garay, G. 2000, ApJ, 531, 861
———. 2002, in preparation
Herbig, G. H. 1998, ApJ, 497, 736
Hodapp, K.-W. 1998, ApJ, 500, L183
Hodapp, K.-W., & Ladd, E. F. 1995, ApJ, 453, 715
Høg, E., Kuzmin, A., Bastian, U., Fabricius, C., Kuimov, K., Lindegren, L., Makarov, V. V., & Roeser, S. 1998, A&A, 335, L65
Jennings, R. E., Cameron, D. H. M., Cudlip, W., & Hirst, C. J. 1987, MNRAS, 226, 461
Keene, J., Davidson, J. A., Harper, D. A., Hildebrand, R. H., Jaffe, D. T., Loewenstein, R. F., Low, F. J., & Pernic, R. 1983, ApJ, 274, L43
Lay, O. P., Carlstrom, J. E., & Hills, R. E. 1995, ApJ, 452, L73
Lefloch, B., Castets, A., Cernicharo, J., Langer, W. D., & Zylka, R. 1998, A&A, 334, 269
Liseau, R., Sandell, G., & Knee, L. B. G. 1988, A&A, 192, 153
Looney, L. W., Mundy, L. G., & Welch, W. J. 2000, ApJ, 529, 477
Moneti, A., & Reipurth, B. 1995, A&A, 301, 721
Moriarty-Schieven, G. H., Powers, J. A., Butner, H. M., Wannier, P. G., & Keene, J. 2000, ApJ, 533, L143
Mundy, L. G., McMullin, J. P., Grossman, A. W., & Sandell, G. 1993, Icarus, 106, 11
Ogura, K. 1995, ApJ, 450, L23
Piché, F., Howard, E. M., & Pipher, J. L. 1995, MNRAS, 275, 711
Reipurth, B. 2000, AJ, 120, 3177
Reipurth, B., Chini, R., Krügel, E., Kreysa, E., & Sievers, A. 1993, A&A, 273, 221
Reipurth, B., Heathcote, S., & Vrba, F. 1992, A&A, 256, 225
Reipurth, B., Rodríguez, L. F., & Chini, R. 1999a, AJ, 118, 983
Reipurth, B., Yu, K. C., Bally, J., & Heathcote, S. 2002, in preparation
Reipurth, B., Yu, K. C., Heathcote, S., Bally, J., & Rodríguez, L. F. 2000, AJ, 120, 1449
Reipurth, B., Yu, K. C., Rodríguez, L. F., Heathcote, S., & Bally, J. 1999b, A&A, 352, L83
Rodríguez, L. F. 1997, in IAU Symp. 182, Herbig-Haro Flows and the Birth of Low-Mass Stars, ed. B. Reipurth & C. Bertout (Dordrecht: Kluwer), 83
Rodríguez, L. F., Anglada, G., & Curiel, S. 1997, ApJ, 480, L125
———. 1999, ApJS, 125, 427
Rodríguez, L. F., Anglada, G., & Raga, A. C. 1995, ApJ, 454, L149
Rodríguez, L. F., et al. 1998, Nature, 395, 355
Rodríguez, L. F., Ho, P. T. P., Torrelles, J. M., Curiel, S., & Cantó, J. 1990, ApJ, 352, 645
Rodríguez, L. F., & Reipurth, B. 1994, A&A, 281, 882
———. 1996, Rev. Mexicana Astron. Astrofis., 32, 27
———. 1998, Rev. Mexicana Astron. Astrofis., 34, 13

Sandell, G., Aspin, C., Duncan, W. D., Russell, A. P. G., & Robson, E. I. 1991, ApJ, 376, L17
Sandell, G., & Knee, L. B. G. 2001, ApJ, 546, L49
Sandell, G., Knee, L. B. G., Aspin, C., Robson, I. E., & Russell, A. P. G. 1994, A&A, 285, L1
Shirley, Y. L., Evans, N. J., Rawlings, J. M., & Gregersen, E. M. 2000, ApJS, 131, 249
Smith, K. W., Bonnell, I. A., Emerson, J. P., & Jenness, T. 2000, MNRAS, 319, 991
Snell, R. L., & Bally, J. 1986, ApJ, 303, 683
Terebey, S., & Padgett, D. L. 1997, in IAU Symp. 182, Herbig-Haro Flows and the Birth of Low-Mass Stars, ed. B. Reipurth & C. Bertout (Dordrecht: Kluwer), 507
Terquem, C., Eislöffel, J., Papaloizou, J. C. B., & Nelson, R. P. 1999, ApJ, 512, L131
Walsh, J. R., Ogura, K., & Reipurth, B. 1992, MNRAS, 257, 110
Wilner, D. J., Myers, P. C., Mardones, D., & Tafalla, M. 2000, ApJ, 544, L69
Wilner, D. J., Reid, M. J., & Menten, K. M. 1999, ApJ, 513, 775
Wolf-Chase, G. A., Barsony, M., & O'Linger, J. 2000, AJ, 120, 1467